Video Article

In Situ Immunofluorescent Staining of Autophagy in Muscle Stem Cells

Francesco Castagnetti[1,2], Elisabetta Fiacco[3], Carol Imbriano[4], Lucia Latella[1,2]

[1]Department of Medicine, Institute of Translational Pharmacology, Italian National Research Council

[2]Epigenetics and Regenerative Medicine, IRCCS Fondazione Santa Lucia

[3]Biological and Environmental Sciences and Engineering Division, King Abdullah University of Science and Technology (KAUST)

[4]Department of Life Sciences, University of Modena and Reggio Emilia

Correspondence to: Lucia Latella at l.latella@hsantalucia.it

URL: https://www.jove.com/video/55908
DOI: doi:10.3791/55908

Keywords: Cellular Biology, Issue 124, Autophagy, muscle stem cells (satellites), muscle regeneration, LC3, MYOD, muscle tissue sections

Date Published: 6/12/2017

Citation: Castagnetti, F., Fiacco, E., Imbriano, C., Latella, L. *In Situ* Immunofluorescent Staining of Autophagy in Muscle Stem Cells. *J. Vis. Exp.* (124), e55908, doi:10.3791/55908 (2017).

Abstract

Increasing evidence points to autophagy as a crucial regulatory process to preserve tissue homeostasis. It is known that autophagy is involved in skeletal muscle development and regeneration, and the autophagic process has been described in several muscular pathologies and age-related muscle disorders. A recently described block of the autophagic process that correlates with the functional exhaustion of satellite cells during muscle repair supports the notion that active autophagy is coupled with productive muscle regeneration. These data uncover the crucial role of autophagy in satellite cell activation during muscle regeneration in both normal and pathological conditions, such as muscular dystrophies. Here, we provide a protocol to monitor the autophagic process in the adult Muscle Stem Cell (MuSC) compartment during muscle regenerative conditions. This protocol describes the setup methodology to perform *in situ* immunofluorescence imaging of LC3, an autophagy marker, and MyoD, a myogenic lineage marker, in muscle tissue sections from control and injured mice. The methodology reported allows for monitoring the autophagic process in one specific cell compartment, the MuSC compartment, which plays a central role in orchestrating muscle regeneration.

Video Link

The video component of this article can be found at https://www.jove.com/video/55908/

Introduction

Skeletal muscle regeneration is the result of the interaction between adult stem cells (Muscle Satellite Cells, MuSCs) and other cell types that are involved in the regenerative process. Muscle homeostasis and functionality are maintained by the combined signals arising from the muscle niche and systemic cues[1,2]. Throughout the lifetime, changes in the MuSC functionality, the muscle niche, and the systemic cues have been reported, leading to the decline of functional capacities in the elderly[3]. MuSCs are set in a niche beneath the basal lamina and, upon muscle injury, are activated to repair damaged muscles[4,5]. In order to ensure a productive regenerative response, it is crucial that MuSCs coordinate different processes necessary for the exit from quiescence, the self-renewal, and the proliferative expansion stage followed by the myogenic differentiation[6]. In the elderly and in muscular chronic diseases, all these functions are compromised, leading to altered muscle functionality[2,3,6,7,8,9,10,11,12,13].

Macroautophagy (referred hereafter as autophagy) is emerging as a crucial biological process essential to preserve tissue homeostasis[14]. The autophagic process encloses trafficking mechanisms, where portions of cytoplasm, organelles, and proteins are engulfed into vesicles that eventually are degraded via the lysosome pathway, promoting the removal of toxic molecules and the recycling of macromolecules. This provides energy-rich compounds to support cell and tissue adaptation under stress or other adverse conditions[15,16]. Together with its cell-survival activity, autophagy can also work as a cell-death inducer, depending upon cell tissue context (*e.g.,* normal versus cancer tissue) and the type of stress stimulus[17,18].

Recent evidence indicates that autophagy is required to maintain muscle mass and myofiber integrity[19,20] and has been reported to be impaired in different muscle dystrophies[21,22,23], including Duchenne Muscular Dystrophy (DMD)[24,25,26,27,28,29,30].Likewise, a progressive reduction of the autophagic process has been observed in the elderly[31,32,33,34,35], after a loss of muscle mass (referred as sarcopenia)[32,33,34,35,36,37], and in myofiber survival[38].

A close relationship between autophagy and the regenerative potential of skeletal muscles was anticipated by a study from Wagers's laboratory, which showed that a calorie restriction enhances MuSC availability and activity[39]. This notion was further supported by the recent observation that the Foxo3-Notch axis activates the autophagic process during self-renewal[40] and the MuSC transition from the quiescent to the proliferating state[41]. These data agree with the progressive reduction of basal autophagy from young to old and geriatric MuSCs, in association with the numerical and functional decline of MuSCs during ageing[42].

In a recent paper, we demonstrated a close relationship between autophagy and the compensatory muscle regeneration that distinguishes the early stages of DMD progression. Accordingly, we observed a reduced autophagic flux at later stages of disease progression, when muscle

regeneration is compromised and fibrotic tissue deposition occurs. Intriguingly, we showed that, in regenerating conditions, autophagy is activated in MuSCs and that modulating the autophagic process impacts MuSC activation and functionality[30].

Altogether, these data highlight the urgency to explore the autophagic process in MuSCs during muscle regeneration in normal and pathological conditions and throughout the life span. Here, we provide a protocol to monitor the autophagic process in MuSCs in muscle regenerative conditions by performing *in situ* immunostaining for microtubule-associated protein 1A/1B-light chain 3 (LC3), a marker of autophagy[43], and MyoD, a marker of myogenic lineage, in muscle tissue sections from control and injured mice. The methodology reported allows for monitoring the autophagic process in one specific cell compartment, the MuSC, which plays a key role in orchestrating muscle regeneration.

Protocol

Mice were bred and maintained according to the standard animal facility procedures, and all experimental protocols were approved by the Animal Welfare Assurance and the internal Animal Research Ethical Committee according to the Italian Ministry of Health and complied with the NIH Guide for the Care and Use of Laboratory Animals.

1. Muscle Injury and the *In Vivo* Block of Autophagic Flux

1. **Muscle injury.**
    1. To induce acute skeletal muscle injury, inject 20 µL of 10 µM cardiotoxin (CTX) stock directly in the left tibialis anterior (TA) muscle of 2 month-old C57BL/6J mice that weigh approximately 20 g. Use an equal number of males and females. Use the unperturbed contralateral limb as a control.
    NOTE: 10 µM CTX in 0.9% sodium chloride solution should be filtered (0.22 µm PVDF filter) and stored at -20 °C. Avoid repeated freeze-thaw cycles.
    2. Using an insulin syringe with a 30 G needle, inject CTX in the middle of the TA. To induce an accurate injury in the TA, ensure that the needle of the syringe enters near the distal tendon, 5 mm deep, from the bottom to the top of the muscle (**Figure 1A**).

2. **Blockade of the autophagic flux in unperturbed and injured mice .**
    1. To assess the autophagic flux, 24 h Post-Injury (p.i.), administer 50 mg/kg chloroquine (CLQ) every 24 h for 4 d by intraperitoneal (IP) injection (**Figure 1B**).
        1. Dissolve CLQ (10 mg/mL) in PBS 1X and filter it through a 0.2 µm membrane. Weigh every mouse and calculate the amount of CLQ to inject.
        NOTE: Prepare and use CLQ solution on the same day. CLQ stock can be stored for up to one month at -20 °C. Since autophagy is a metabolic-related process, always perform CLQ treatment always at the same time (*i.e.* in the morning before 10 AM).

2. Muscle Tissue Sections

1. **Mouse sacrifice.**
    1. Euthanize the mice 5 days after the injury.
    2. Perform euthanasia by cervical dislocation or by CO_2 (to be followed by cervical dislocation for confirmation). Since the autophagy process is related to mouse sleeping/eating habits, always sacrifice the mice at the same time, preferably in the morning (*i.e.* before 10 AM).

2. **TA isolation and inclusion.**
    1. Before the dissection, spray the mouse with 70% ethanol.
    2. Using scissors make a small, perpendicular incision (3 mm long) on the dorsal skin of the mouse at the level of the hips. Cut the tail and the feet to simplify the skin removal. Pull the skin towards the tail and remove it to expose the underlying muscles; the TA muscle is easy to localize, as shown in **Figure 2A**.
    3. With the help of two forceps, grasp the distal tendons.
    4. Cut the distal tendons; the TA and extensor digitorium longus (EDL) tendons are often cut jointly and later separated (see step 2.2.6).
    5. Using forceps, hold the TA muscle by the tendon and carefully pull the muscle up toward the proximal end (near the knee; **Figure 2B**).
    NOTE: At this point, the EDL and TA muscles are readily recognizable, the TA being larger and more superficial than the EDL.
    6. Separate the TA from the EDL muscle by pulling the two distal tendons in the opposite directions (**Figure 2C**).
    7. Cut the proximal tendon.
    8. Using forceps, remove the thin fascia that covers the muscle, without damaging the tissue.
    9. Remove excessive moisture in the sample with the help of a paper towel. Ensure that the muscle is neither wet, nor excessively dry, as excessive moisture will produce significant damage to the muscle and jeopardize the next staining.
    10. Place Optimal Cutting Temperature (OCT) compound at the bottom of a mold and place the muscle into it, in the orientation shown in **Figure 2D**. Add 100% isopentane to a beaker until it reaches a depth of approximately 3-4 cm. Place the beaker in contact with liquid nitrogen in a polystyrene box.
    11. Do not let the liquid nitrogen enter the beaker, as it will produce a bubbling foam, which can affect the inclusion and damage the muscle sections.
    12. Observe the isopentane and wait until it reaches the proper temperature (between -140 °C and -150 °C); at the appropriate temperature, a solid white layer of frozen isopentane will crystallize on the bottom of the beaker.
    13. If the isopentane entirely freezes solid, melt and chill it to freezing temperature before proceeding to the next step.

14. Using prechilled forceps, delicately lower the mold into the isopentane for approximately 20-30 s. Place the frozen sample into a container with dry ice until it is transferred to a -80 °C freezer.
    NOTE: The protocol can be paused here.

3. **Muscle tissue cryosections.**
    1. After at least one night at -80 °C, perform cryosectioning.
    2. Take the cryostat knife and the anti-roll plate out of the -20 °C freezer and place them on the respective supports into the cryostat cabinet.
    3. Put a drop of OCT on the sample stub and place on it the frozen sample, in vertical N-S orientation, as visualized in **Figure 2D**.
    4. Place the sample stub on the chuck.
    5. Without pulling the anti-roll plate down on the knife, make some cuts at 40 µm to get rid of OCT that does not include muscle. When the muscle becomes visible, reduce the slice thickness to 7-8 µm.
    6. Pull down the anti-roll plate until it is aligned with the edge of the knife or a little above it.
    7. Cut transversal sections 7-8 µm thick and mount 3-4 slices per histological slide.
       NOTE: The suggested cryostat temperature is between -15 °C and -23 °C. Cross-sections of the samples are needed for the subsequent analysis to pinpoint the muscle stem cells in the satellite niche position.
    8. To maximize the adherence of the section, keep the slides at room temperature for 10-15 min so to prevent their detachment during antibody incubation.
       NOTE: The air-drying step could affect immunostaining, providing ambiguous results. Slides can be stored unfixed for several months at -80 °C. The protocol can be paused here.

4. **Checking for muscle damage in cryosections of TA muscles by performing Hematoxylin Eosin (H&E) staining.**
    1. To evaluate the quality of the muscle (*i.e.* the effectiveness of the injury, muscle isolation and inclusion, and cryosections), perform an H&E staining. For every experimental time point, fix one slide with 4% PFA for 10 min. After fixation, wash the slides well in several changes of 1x PBS.
       NOTE: Caution. PFA is carcinogen and must be handled carefully.
    2. Take one slide for every experimental point and put them in a staining jar.
    3. Fill the jar with 9 g/L hematoxylin until the sections are covered and incubate for 8 min.
    4. Recycle the hematoxylin.
    5. Leave the jar under running water for 10 min to remove the excess of hematoxylin.
       NOTE: Make sure not to flow the water directly onto the sections.
    6. Wash using sterilized water.
    7. Incubate the sections with eosin 0.5% (w/v) in acidified 90% ethanol for 1 min.
    8. Recycle the eosin.
    9. Wash twice with sterile water for 3 min/wash.
       NOTE: Perform the following steps at a chemical hood.
    10. Wash the sections with 70% ethanol.
    11. Wash the sections with 90% ethanol.
    12. Wash the sections with 100 % ethanol.
    13. Incubate the sections with 0.879 g/mL o-Xylene.
        NOTE: Caution. o-Xylene is flammable and moderately toxic. Manipulate it under chemical hood, wearing protective equipment, including gloves, a lab coat, and a mask.
    14. Recycle the o-Xylene.
    15. Put the slides over a piece of paper to dry.
    16. Close the slides using a quick-hardening, xylene-based mounting medium.
    17. Check the quality of the sections under an optical microscope at 10X magnification (see **Figure 3**)
        NOTE: The protocol can be paused here.

3. Immunostaining for LC3 and MyoD in Injured Muscle Tissue Sections

1. **Fixation of muscle tissue sections.**
    1. Prepare an incubation chamber by wetting a piece of paper and placing it on the bottom of a closable plastic box to maintain a high level of humidity inside the chamber. Fix tissue sections with 4% paraformaldehyde (PFA) in 1x PBS for 10 min.
       NOTE: A wet piece of paper is used to avoid drying the sample. Prepare fresh PFA or use PFA stored at -20 °C. Caution. PFA is toxic; the powder must be handled with care when making the stock solution. This operation must be performed at a chemical hood, with protective equipment, including gloves, a lab coat, and a mask. Also, when in solution, the PFA should be manipulated carefully.
    2. Remove the PFA and wash the sections with 1x PBS for 5-7 min; repeat this step 3 times.

2. **Permeabilization of muscle tissue sections.**
    1. Draw a hydrophobic barrier around the tissue sections using a pap pen.
       NOTE: This step defines the surface around the tissue sections and minimizes the volume of antibodies described in steps 3.4, 3.6, 3.7, and 3.9.
    2. Cover the sections with 200 µL of cold (-20 °C) methanol and put the incubation chamber horizontally inside a freezer at -20 °C for 5 min .
    3. Remove the incubation chamber from the freezer, aspirate the methanol, and wash the sections with1X PBS for 5-7 min at RT; repeat this step 3x.

3. **Blocking**
    1. Prepare a fresh block solution of 4% Bovine Serum Albumin (BSA) in PBS 1x.

NOTE: BSA solution can be stored up for 1 week at 4 °C.
2. Incubate the sections with block solution for at least 60 min at RT.
3. Remove the blocking solution.
4. Prepare 100 µL of anti-Fab mix by diluting 20 µg/mL anti-Fab in 1x PBS. Incubate the sections with an unconjugated affinity-purified F(ab) fragment of anti-mouse IgG for 1 h at RT.

4. **Primary antibody incubation.**
   1. Prepare 100 µL of primary antibody mix for each slide by dissolving LC3 and MyoD antibodies in 4% BSA in 1x PBS. Use 5 µg/mL of anti-LC3 (rabbit polyclonal antibody) and 10 mg/L of anti-MyoD (mouse monoclonal antibody). Incubate the primary antibody mix overnight at 4 °C.

5. **Washes.**
   1. Remove the primary antibody mix.
   2. Wash the sections with 1% BSA in 1X PBS for 10 min; repeat this step 3x.

6. **Secondary antibody incubation.**
   1. Prepare 100 µL of secondary antibody mix for each slide. Dissolve goat anti-rabbit 488 (5 µg/mL) and goat anti-mouse 594 (5 µg/mL) in 4% BSA in 1x PBS.
      NOTE: Avoid excessive exposure to light to prevent fluorochrome bleaching. Perform the following steps in the dark.
   2. Incubate the sections with the secondary antibody mix for 45 min at RT.
   3. Remove the secondary antibody mix and wash the sections with 1x PBS for 5-7 min; repeat this step 3x.

7. **Primary antibody incubation.**
   1. Dilute laminin-2 (α-2-chain) monoclonal antibody (0.33 µg/mL) in 4% BSA in 1x PBS using 100 µL of mixture for each slide. Incubate the sections in the primary antibody mix for 1-2 h at RT.

8. **Washes.**
   1. Remove the primary antibody mix.
   2. Wash the sections with 1% BSA in 1X PBS for 10 min; repeat this step 3x.

9. **Secondary antibody incubation.**
   1. Prepare 100 µL of secondary antibody mix for each slide by diluting goat anti-rat 647 (5 µg/mL) in 4% BSA in 1X PBS. Incubate the sections in secondary antibody mix for 45 min at RT.
   2. Remove the secondary antibody mix and wash the sections with 1x PBS for 5-7 min; repeat this step 3x.

10. **4',6-Diamidino-2-phenylindole (DAPI) incubation.**
    1. Add 200 µL of 300 nM DAPI solution in 1x PBS to each slide. Incubate for 5 min at RT. Store the DAPI solution at 4 °C in the dark.
    2. Wash the sections with 1x PBS for 5-7 min; repeat this step 3x.

11. **Mounting stained muscle sections.**
    1. Remove the excess of washing solution from the sections.
    2. Place 10 µL of glycerol in 1x PBS (3:1) on the stained sections in the middle of the slide and add a coverslip, avoiding the formation of air bubbles.

4. Confocal Microscopy Acquisition

1. Acquire the images using a four-laser confocal microscope integrated with an image capture system and analytical software.
   NOTE: MyoD is conjugated with a 594 dye that is a bright red-fluorescent dye, with excitation ideally suited to the 594 nm laser (excitation: 590 nm, emission: 617 nm). LC3 is conjugated with a 488 dye that is a bright green-fluorescent dye, with excitation ideally suited to the 488 nm laser line (excitation: 495 nm, emission: 519 nm). Laminin is conjugated with a 647 dye that is a bright far-red-fluorescent dye, with excitation ideally suited to the 647 nm laser line (excitation: 650 nm, emission: 668 nm).
2. Place the slides in the microscope tray and use 63X magnification to detect nuclear signals.Manually focus on the regenerative areas by centering the fields of active regeneration, relying on muscle morphology (see **Figure 4**).
   NOTE: While in unperturbed muscle, myofiber size is virtually constant (**Figure 4A**), injury-mediated muscle regeneration can be recognized by the appearance of smaller myofibers, which are the newly formed fibers after regeneration. Moreover, the muscle in active regeneration is characterized by an extensive infiltrate that is made of macrophages, fibro-adipogenic precursors, and cells that are localized to the damaged muscles to orchestrate muscle regeneration (**Figure 4B**).
3. Evaluate the immunofluorescent staining in regenerative areas by focusing on MuSCs that are located under the basal lamina of the myofibers.
4. Focus on MuSCs that are positive for MyoD staining and positioned within myofibers marked by laminin staining (see **Figure 4B**, white arrows).
5. Use at least 3 mice/experimental group and use the microscope to acquire 63X magnification images of at least 7 fields for each experimental group.
6. **Once the regenerative areas are identified, focus using the DAPI staining and then adjust the other single channels.**
   1. Use the following microscope settings: Channel A594 Pinhole 1.2 Airy Unit, Gain 791; Channel A488 Pinhole 1.6 Airy Unit, Gain 659; Channel A647 Pinhole 1.4 Airy Unit, Gain 719.

7. After adjusting the focus of the single channels, proceed to acquire the images at a 1,024 x 1,024 frame size and a 12.61 µs pixel dwell.
8. Count the percentage of MyoD-positive cells (control for the correct location under the lamina) that are LC3-negative and the percentage of MyoD-positive cells that display an LC3 signal.

NOTE: The percentage of MyoD-positive cells that exhibit LC3 staining is the readout of this protocol.

Representative Results

This protocol describes an efficient *in situ* method to detect autophagy in MuSCs during muscle regeneration.

CTX *In Vivo* Treatments:

Use CTX to induce muscle damage in TA muscles and use unperturbed muscles as controls. Since autophagy is highly dynamic, block the autophagic flux by performing IP injections of CLQ (**Figure 1**). CLQ treatment is essential to assess whether the autophagic flux is active or is kept at basal levels.

Tibialis Anterior Isolation:

Isolate the TA muscle, as described in **Figure 2**, and place it in a mold chamber in N-S orientation to subsequently obtain transversal muscle tissue sections. This step is crucial to attain sections and to identify MuSCs in the proper location beneath the myofiber basal lamina.

Hystological Examination of CTX-induced Muscle Damage

Verify that muscle injury occurred by performing histological staining. Perform H&E staining and check under 10X magnification: while unperturbed muscles display generally invariable myofiber sizes, the typical features of injured muscles include the disruption of myofibers that are different in size and abundant inflammatory infiltrate. Another parameter to confirm that the regenerative process is taking place is the centro-nucleation of the myofibers, which is absent in unperturbed muscles and is a sign of the formation of new fibers in mice undergoing active regeneration (**Figure 3**).

Autophagy is Coupled to MyoD-positive Cells During Muscle Regeneration:

Perform immunofluorescent staining to detect MuSCs, identified as MyoD-positive, that display an LC3 signal. Laminin staining is helpful to locate MuSCs in the proper position in the niche beneath the basal lamina (**Figure 4**). Autophagic basal levels distinguish unperturbed skeletal muscles and significantly increase in coincidence with muscle regeneration[30]. Accordingly, uninjured mice do not show any MuSC activation, detected by the absence of MyoD-positive cells and no LC3 signal. Conversely, upon muscle damage, MyoD-positive MuSCs become positive for LC3, demonstrating that the autophagic process is activated during muscle regeneration in activated satellite cells.

During the initial stages of the regenerative response, different cellular types localize to the site of the lesion, including inflammatory cells and fibro-adipogenic precursors, making the injured area densely overcrowded. It is crucial to distinguish between all different cellular types, focusing on the MuSC location underneath the myofiber lamina and relying on MyoD positivity.

In basal conditions, LC3 is expressed ubiquitously and is barely detected by immunofluorescence. As a result of elevated autophagy, this staining pattern changes and become detectable mainly in the cytoplasm. When evaluating MyoD/LC3 staining, consider that MuSCs are small cells and that the cytoplasmic region is limited; this why LC3 may look perinuclear.

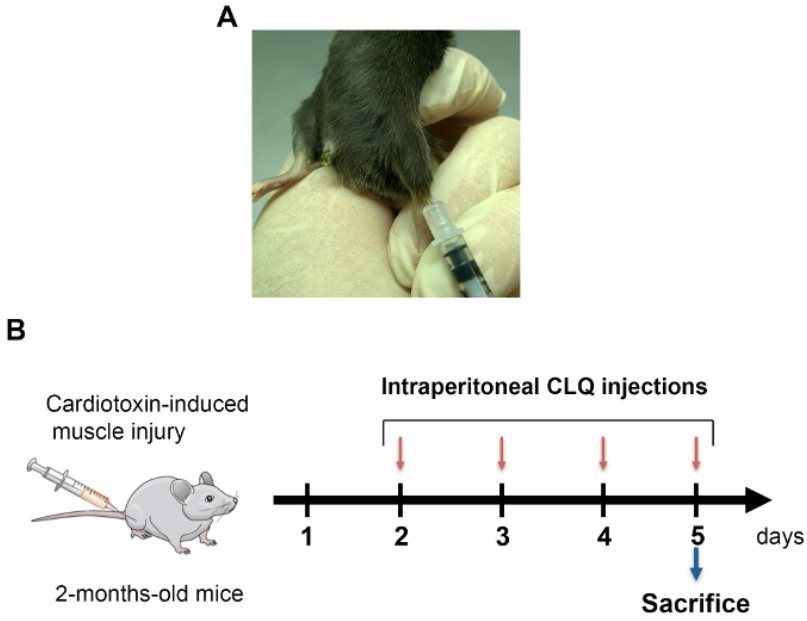

Figure 1: CTX *In Vivo* Treatments. (**A**) To induce muscle damage, inject 10 µL of 10 µM CTX directly in the left TA muscles of 2-month-old WT mice. Use the contralateral limb as a control. (**B**) Schematic representation of cardiotoxin-induced muscle injury. 24 h post-injury, treat the mice with intraperitoneal injections of 50 mg/kg CLQ every 24 h for 4 days and then sacrifice the animals. Use untreated uninjured and injured mice as controls. This protocol allows for the study of the involvement of the autophagic process during muscle regeneration. Please click here to view a larger version of this figure.

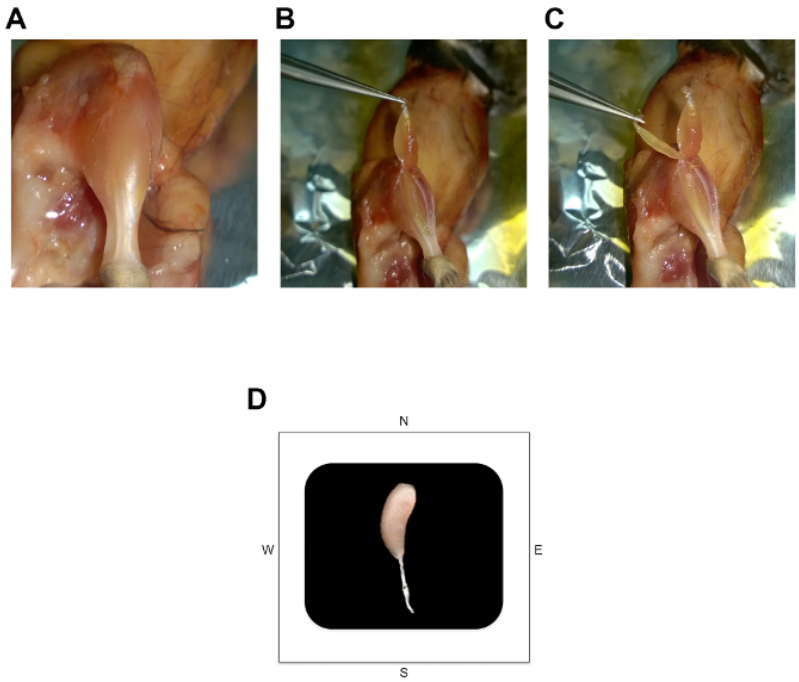

Figure 2: TA Isolation. (**A**) Representative image of the TA as it looks before isolation. (**B**) After cutting the distal tendon, hold the TA muscle by the tendon and carefully pull the muscle up toward the proximal end (near the knee). (**C**) Discriminate the EDL from the TA muscle, which is larger and more superficial than the EDL. Separate the TA from the EDL muscle by pulling the two distal tendons in opposite directions. (**D**) Once the TA is isolated, place it in the mold chamber, as described, in N-S orientation. Please click here to view a larger version of this figure.

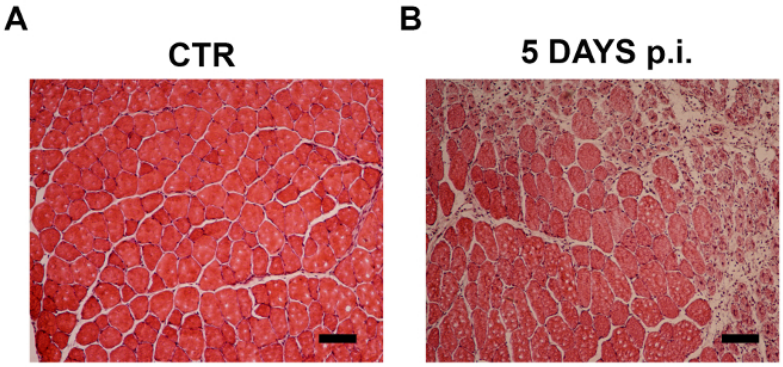

Figure 3: CTX Induces Muscle Damage. Representative images of H&E staining on TA transversal tissue sections from control, uninjured (**A**) and 5 d p.i. (**B**) WT mice. H&E staining reveals normal fiber morphology in control mice (**A**) and massive muscle damage and infiltrate in injured muscles (**B**), demonstrating an impaired morphology upon CTX injection. Scale bar = 50 µm. Please click here to view a larger version of this figure.

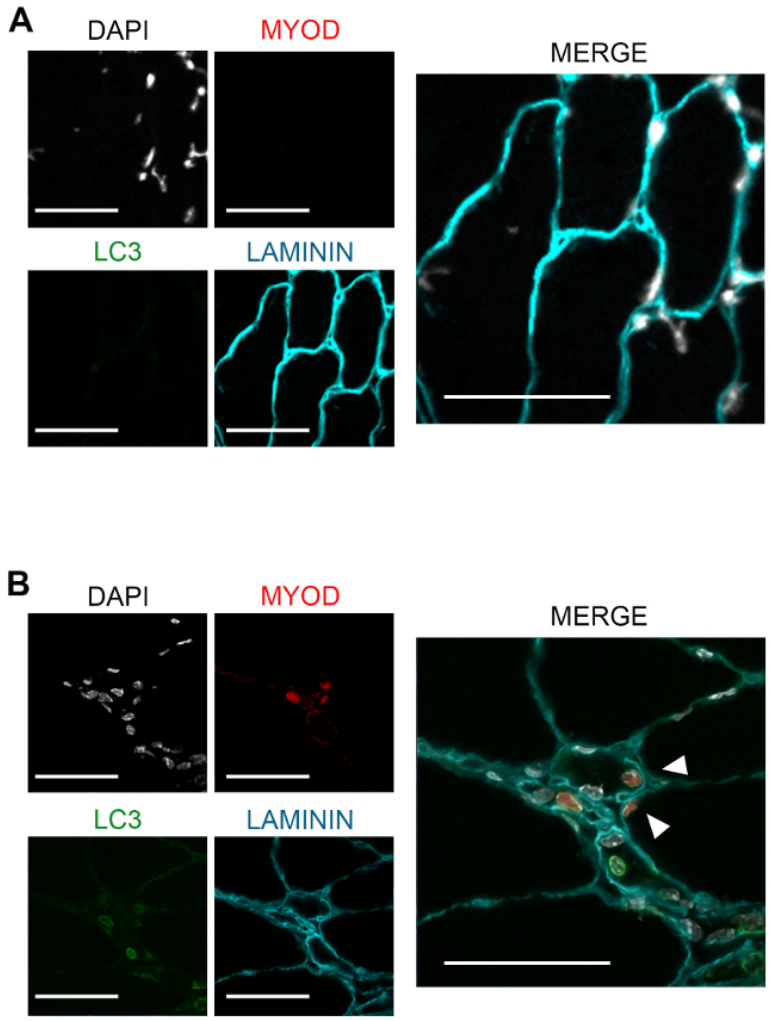

Figure 4: Autophagy is Coupled to MyoD-positive Cells during Muscle Regeneration. Representative images of TA sections from control (**A**) and injured (**B**) WT mice immunostained with LC3 (green) and MyoD (red). Laminin (cyan) staining marks muscle fibers, and nuclei are counterstained with DAPI (white). The right panels show representative images of the merge signal. White arrows indicate satellite cells that are beneath the basal lamina of the fiber marked by laminin staining. The following protocol allows for measuring autophagy through LC3 staining in muscle stem cells undergoing myogenic lineage, marked by MyoD. Scale bar = 50 µm. Please click here to view a larger version of this figure.

Discussion

This protocol describes how to monitor autophagy in skeletal muscle stem cells during compensatory muscle regeneration. Several antibodies for the co-staining of LC3 and MyoD were tried, and the ones that work in mouse tissue sections and create successful results are listed here (see **Materials Table**). The permeabilization with methanol (see step 3.2.2) is highly recommended for successful staining.

The limitation of this protocol is linked to the intrinsic variability of the mice, which compels the use of at least 3 mice/experimental group.This methodology reflects a step forward in the study of autophagy during skeletal muscle regeneration, as the majority of results up to now were made in isolated cells. The *in situ* analysis allowed for the study of autophagy in the natural environment, without the need of a cell isolation that might affect metabolic processes, such as autophagy.

Given the highly dynamic nature of the autophagic process, the CLQ treatments are a critical step to monitoring the autophagic process *in vivo*. CLQ blocks the later stages of the autophagic process, leading to LC3 accumulation when autophagy is sustained. Therefore, CLQ treatment makes LC3 detectable by *in situ* examination. In unperturbed skeletal muscles, the basal autophagic process is not further increased by CLQ treatment, as revealed by the absence of detectable LC3 accumulation. However, in regenerating muscles, LC3 accumulates upon CLQ treatment, demonstrating autophagic activation. A critical step is to sacrifice the mice at the same time in the morning (*i.e.* at 10 AM). Another critical step in the protocol is the identification of MuSC, which must not be interchanged with another cellular type that populates damaged

muscle during the regenerative response. The identification of MuSCs under the basal lamina that display MyoD positivity is the key to focus on satellite cells.

In summary, we present a suitable *in situ* method to detect the involvement of the autophagic process in MuSCs. This technique can serve as the basis for tests of pharmacological approaches to autophagy modulation, which might be used to improve skeletal muscle regeneration in normal and pathological conditions.

Disclosures

The authors have nothing to disclose

Acknowledgements

This work was supported by NIAMS AR064873, Epigen Project PB. P01.001.019/Progetto Bandiera Epigenomica IFT to L.L.

References

1. Bentzinger, C.F., et al. Differential response of skeletal muscles to mTORC1 signaling during atrophy and hypertrophy. *Skelet Muscle.* **3**(1), 6 (2013).
2. Chakkalakal, J.V., et al. The aged niche disrupts muscle stem cell quiescence. *Nature.* **490**(7420), 355-60 (2012).
3. Jang, Y.C., et al. Skeletal muscle stem cells: effects of aging and metabolism on muscle regenerative function. *Cold Spring Harb Symp Quant Biol.* **76**, 101-11 (2011).
4. Cheung, T.H., Rando, T.A. Molecular regulation of stem cell quiescence. *Nat Rev Mol Cell Biol.* **14**(6), 329-40 (2013).
5. Collins, C.A., Partridge, T.A. Self-renewal of the adult skeletal muscle satellite cell. *Cell Cycle.* **4**(10), 1338-41 (2005).
6. Bentzinger, C.F., et al. Cellular dynamics in the muscle satellite cell niche. *EMBO Rep.* **14**(12), 1062-72 (2013).
7. Bernet, J.D., et al. p38 MAPK signaling underlies a cell-autonomous loss of stem cell self-renewal in skeletal muscle of aged mice. *Nat Med.* **20**(3), 265-71 (2014).
8. Cosgrove, B.D., et al. Rejuvenation of the muscle stem cell population restores strength to injured aged muscles. *Nat Med.* **20**(3), 255-64 (2014).
9. Sousa-Victor, P., et al. Geriatric muscle stem cells switch reversible quiescence into senescence. *Nature.* **506**(7488), 316-21 (2014).
10. Madaro, L., Latella, L. Forever young: rejuvenating muscle satellite cells. *Front Aging Neurosci.* **7**, 37 (2015).
11. Price, F.D., et al. Inhibition of JAK-STAT signaling stimulates adult satellite cell function. *Nat Med.* **20**(10), 1174-81 (2014).
12. Tierney, M.T., et al. STAT3 signaling controls satellite cell expansion and skeletal muscle repair. *Nat Med.* **20**(10), 1182-6 (2014).
13. Judson, R.N., Zhang, R.H., Rossi, F.M. Tissue-resident mesenchymal stem/progenitor cells in skeletal muscle: collaborators or saboteurs? *FEBS J.* **280**(17), 4100-8 (2013).
14. Kroemer, G., Marino, G., Levine, B. Autophagy and the integrated stress response. *Mol Cell.* **40**(2), 280-93 (2010).
15. Marino, G., Madeo, F., Kroemer, G. Autophagy for tissue homeostasis and neuroprotection. *Curr Opin Cell Biol.* **23**(2), 198-206 (2011).
16. Jiang, P., Mizushima, N. Autophagy and human diseases. *Cell Res.* **24**(1), 69-79 (2014).
17. Eskelinen, E.L. Doctor Jekyll and Mister Hyde: autophagy can promote both cell survival and cell death. *Cell Death Differ.* **12 Suppl 2**, 1468-72 (2005).
18. Basile, V., et al. bis-Dehydroxy-Curcumin triggers mitochondrial-associated cell death in human colon cancer cells through ER-stress induced autophagy. *PLoS One.* **8**(1), e53664 (2013).
19. Neel, B.A., Lin, Y., Pessin, J.E. Skeletal muscle autophagy: a new metabolic regulator. *Trends Endocrinol Metab.* **24**(12), 635-43 (2013).
20. Sandri, M. Autophagy in skeletal muscle. *FEBS Lett.* **584**(7), 1411-6 (2010).
21. Grumati, P., et al. Autophagy is defective in collagen VI muscular dystrophies, and its reactivation rescues myofiber degeneration. *Nat Med.* **16**(11), 1313-20 (2010).
22. Chrisam, M., et al. Reactivation of autophagy by spermidine ameliorates the myopathic defects of collagen VI-null mice. *Autophagy.* **11**(12), 2142-2152 (2015).
23. Grumati, P., et al. Autophagy induction rescues muscular dystrophy. *Autophagy.* **7**(4), 426-8 (2011).
24. De Palma, C., et al. Autophagy as a new therapeutic target in Duchenne muscular dystrophy. *Cell Death Dis.* **3**, e418 (2012).
25. Hindi, S.M., et al. Distinct roles of TRAF6 at early and late stages of muscle pathology in the mdx model of Duchenne muscular dystrophy. *Hum Mol Genet.* **23**(6), 1492-505 (2014).
26. Pauly, M., et al. AMPK activation stimulates autophagy and ameliorates muscular dystrophy in the mdx mouse diaphragm. *Am J Pathol.* **181**(2), 583-92 (2012).
27. Spitali, P., et al. Autophagy is Impaired in the Tibialis Anterior of Dystrophin Null Mice. *PLoS Curr.* **5** (2013).
28. Whitehead, N.P. Enhanced autophagy as a potential mechanism for the improved physiological function by simvastatin in muscular dystrophy. *Autophagy.* **12**(4), 705-706 (2016).
29. Whitehead, N.P., et al. A new therapeutic effect of simvastatin revealed by functional improvement in muscular dystrophy. *Proc Natl Acad Sci U S A.* **112**(41), 12864-9 (2015).
30. Fiacco, E., et al. Autophagy regulates satellite cell ability to regenerate normal and dystrophic muscles. *Cell Death Differ.* **23**(11), 1839-1849 (2016).
31. Lee, I.H., et al. A role for the NAD-dependent deacetylase Sirt1 in the regulation of autophagy. *Proc Natl Acad Sci U S A.* **105**(9), 3374-9 (2008).
32. Rubinsztein, D.C., Marino, G., Kroemer, G. Autophagy and aging. *Cell.* **146**(5), 682-95 (2011).
33. Colman, R.J., et al. Caloric restriction delays disease onset and mortality in rhesus monkeys. *Science.* **325**(5937), 201-4 (2009).
34. Levine, B.,Kroemer, G. Autophagy in the pathogenesis of disease. *Cell.* **132**(1), 27-42 (2008).

35. Yang, L., et al. Long-Term Calorie Restriction Enhances Cellular Quality-Control Processes in Human Skeletal Muscle. *Cell Rep.* **14**(3), 422-8 (2016).
36. Wenz, T., et al. Increased muscle PGC-1alpha expression protects from sarcopenia and metabolic disease during aging. *Proc Natl Acad Sci USA.*, **106**(48), 20405-10 (2009).
37. Carnio, S., et al. Autophagy Impairment in Muscle Induces Neuromuscular Junction Degeneration and Precocious Aging. *Cell Rep.* (2014).
38. Sandri, M., et al. Misregulation of autophagy and protein degradation systems in myopathies and muscular dystrophies. *J Cell Sci.* **126**(Pt 23), 5325-33 (2013).
39. Cerletti, M., et al. Short-term calorie restriction enhances skeletal muscle stem cell function. *Cell Stem Cell.* **10**(5), 515-9 (2012).
40. Gopinath, S.D., et al. FOXO3 promotes quiescence in adult muscle stem cells during the process of self-renewal. *Stem Cell Reports.* **2**(4), 414-26 (2014).
41. Tang, A.H., Rando, T.A. Induction of autophagy supports the bioenergetic demands of quiescent muscle stem cell activation. *EMBO J.* **33**(23), 2782-97 (2014).
42. Garcia-Prat, L., et al. Autophagy maintains stemness by preventing senescence. *Nature.* **529**(7584), 37-42 (2016).
43. Klionsky, D.J., et al. Guidelines for the use and interpretation of assays for monitoring autophagy (3rd edition). *Autophagy.* **12**(1), 1-222 (2016).

